Interferences in the Transverse Profile of a Toluene Beam Induced by a Resonant RF Electric Field†

M. Morato, J. O. Cáceres, A. G. Gonzálvez, and A. González Ureña*

Unidad de Láseres y Haces Moleculares, Instituto Pluridisciplinar, Universidad Complutense de Madrid, Madrid 28040, Spain

Received: March 31, 2009; Revised Manuscript Received: June 1, 2009

In this work, the interaction of a supersonic beam of toluene diluted in He with a resonant oscillating RF field is investigated both experimental and theoretically. It is shown how the resonant field induces a peak structure in the transverse beam profile which can be explained by the onset of molecular interferences. Specifically, the interaction of a toluene beam of 0.12 eV of translational energy with a resonant RF field of 1.12 kV/m amplitude, and −610 kV/m^2 of gradient at the horizontal plane, during 160 μs produces a series of maxima in the transverse beam profile. The observed structure was satisfactorily reproduced by a quantum interference model based on the interaction of two coherent superpositions induced by the resonant RF field. It appears the present experimental technique could be useful to investigate the spectroscopy and dynamical behavior of coherent beams of polar molecules.

Introduction

Since the first experimental demonstration of molecule interference by Estermann and Stern[1] in 1930, which showed the diffraction of H_2 at a LiF crystal surface, it was only during the past decade of the 20th century when additional experiments with diatomic molecules reported advances in molecular interferometry. Thus, a Ramsey−Bordé interferometer was realized for the iodine dimer in 1994[2] and was later used[3] for K_2. Moreover, a mechanical Mach−Zehnder interferometer was demostrated[4] for Na_2, and the analog to the Mach−Zehnder interferometer, a Talbot−Lau interferometer, was later applied to experiments, with Li_2.[5] Furthermore, diffraction at nanofabricated gratings proved the existence of the weakly bound helium dimer[6] and was used to measure its binding energy.[7] More recently, diffraction experiments with these nanofabricated objects were carried out to show the wave−particle duality of not only He clusters[8] but also molecules as large as C_{60}^9 or C_{70}^{10}.[9,10]

In all above experiments, interferences were originated by the superposition of molecular external states. Likewise, in the classical two-slit Young experiment, due to the associated molecular de Broglie wavelength, the two physically different paths accumulate a distinct phase leading to interferences when they recombine at the detector. Unlike the previous experiments, the present work reports on molecular interferences due to a superposition of internal states where their distinct phases are originated by the interaction of the toluene molecular dipole with a resonant RF field.

The interaction of polar molecules with resonant RF electric fields is a subject currently investigated by our group using different experimental methodologies.[11−15] Thus, depletion spectra of molecular beams have been reported when such polar molecules interact with static and resonant RF fields.[11−15] More recently, beam splitting of 1.5 mm toward both the positive and negative direction perpendicular to the beam propagation axis of a supersonic toluene beam seeded in He was reported[15] as a result of its resonant interaction with a RF electric field. The observed toluene beam splitting could be explained by the onset of molecular interferences induced by the resonant RF field.[16]

In this work, the interaction of a supersonic beam of toluene diluted in He with a resonant oscillating RF field is revisited under better experimental conditions. It is shown how the resonant field induces a peak structure in the transverse beam profile which can be well explained by molecular interferences. As mentioned further below, in the present investigation, the molecular interferences are due to a superposition of internal (J, K, and M) states first split by a static DC field and, then, coherently coupled by a resonant RF field given by $E(t) = E_1 \cos \omega_0 t$. In a previous work,[17] it was demonstrated that the interaction of a polar molecule with a resonant RF field induced two coherent superpositions whose phase shift depends on distinct parameters characterizing the molecule−field interaction as, for example, the molecule's dipole moment, the strength of the RF field, and the interaction time.

Indeed, because of the experimental implementation, the amplitude E_1 of the RF field changes along the perpendicular direction of the beam propagation axis. Thus, for a given resonant angular frequency ω_0 and interaction time t, the RF field varies along the perpendicular direction and, consequently, also the interaction energy between the molecular dipole moment and the RF field. As a result, the molecular wave function shows a distinct phase along this perpendicular direction, leading to an interference pattern in the transverse beam profile.

We believe the present results constitute the first experimental report where molecular interferences are evidenced in the transverse profile of a beam whose polar molecules interact with an RF electric field. Indeed, our results indicate how the employed experimental approach constitutes an easy and direct methodology to produce coherent beams of polar molecules, whose spectroscopy and dynamical behavior could be investigated. We also believe our simple molecular beam technology could be used to control molecular processes.

† Part of the "Vincenzo Aquilanti Festschrift".

* Corresponding author. E-mail: laseres@pluri.ucm.es.

10.1021/jp902928e
Published on Web 07/01/2009

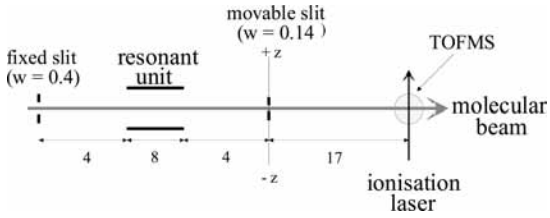

Figure 1. Simplified sketch of the experimental layout. A supersonic beam of toluene travels inside a static and an oscillating RF field. Using the laser ionization coupled to the time-of-flight spectrometer, two transverse beam profiles are taken by moving the final slit along the *z*-axis. The *on* or *off* profile corresponds to the case in which the frequency is *on* or *off* resonance with the energy splitting produced by the static DC field. All dimensions in cm. The distance from the nozzle to the first collimator (shown at the left) is 32 cm. The nominal full beam divergence is 2.8×10^{-3} rad.

Experimental Method and Molecule−Field Interaction Conditions

The main features of the experimental methodology have been described elsewhere,[14,15] and only a brief description is given here. The present experiment employs a supersonic beam of toluene produced by bubbling 3 bar of He through liquid toluene at 0 °C. The volatile impurities were removed from the toluene through freeze and thaw cycles. The supersonic expansion occurs through a nozzle of 0.5 mm of diameter, with the rest of the conditions those described in ref 15. For a better understanding of the beam geometry and collimation, a simplified layout of the experimental setup is shown in Figure 1.

At the final ionization region, the beam divergence is determined by the last slit width of 0.14 cm located 48 cm from the nozzle. The present experimental conditions give a full nominal beam divergence of $\leq 2.8 \times 10^{-3}$ rad.[18]

Strictly speaking, the experimental investigation carried out in the present work does not require a very small beam divergence for the onset of molecular interferences (see the Data Analysis and Discussion section). The basic requirement is that the beam experiences a *z*-dependent RR field amplitude.

Thus, the beam divergence requirement essentially stems from the employed detection geometry. Due to experimental limitations, the ionization laser is directed along the perpendicular direction to the beam axis. Therefore, unless one uses a narrow (movable) slit, the ionization signal would reflect the integral measurement of the whole profile and, consequently, the interferences, produced by the nonhomogeneous RF field, would not manifest.

As the polar molecule travels inside the RF unit, the C-field, first the applied DC field splits any (J, K) state into its $2J + 1$ sublevels characterized by the M_J value; right after, an oscillating RF field is turned on which can produce coherent superpositions when the RF frequency is resonant with the (J, K, M) Stark splitting.

For the understanding of the resonant interaction here employed, we shall recall that when a molecule with a permanent electric dipole moment, μ, interacts with a homogeneous static Stark field, with E as the field strength the energy of the molecule is perturbed and given by[19−21]

$$W = W_0 + W_{\text{Stark}} \tag{1}$$

in which W_0 is the energy of the unperturbed system (i.e., when $E = 0$) and $W_{\text{Stark}} = -\bar{\mu}_E E$. Here, $\bar{\mu}_E$ is the mean component of the electric moment in the field direction. If the linear molecule is in a Σ state, the dipole moment is perpendicular to the total angular momentum (we neglect spin effects) and therefore $\bar{\mu}_E = 0$. In other works, there is no first order Stark splitting.[21] However, there is a second order effect when one considers the action of the Stark field on the molecular rotation.

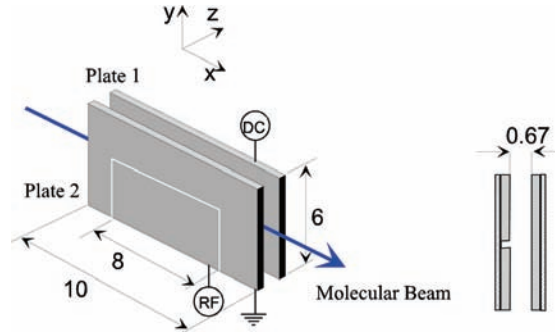

Figure 2. Schematic view of the C-field unit: (left) perspective view including the DC and RF field connection; (right) front view in the *yz* plane. All dimensions in cm.

For a symmetric top molecule, $\bar{\mu}_E$ is no longer zero and a linear Stark effect arises given by[19−21]

$$W_{\text{Stark}} = -\mu E \frac{KM}{J(J+1)} \tag{2}$$

Here, μ is the permanent electric dipole moment which in the case of the toluene molecule equals $\mu = 0.375D$,[22] J is the total angular momentum, K is the magnitude of the projection of J on the internuclear axis, and M is the projection of J on the space fixed axis, i.e., the direction of the static E field. In this work, we restrict ourselves to the $J = K = 1$ case of the electronic ground state. Consequently, the Stark interaction is given by

$$W_{\text{Stark}} = -\mu E \frac{M}{2} \tag{3}$$

Thus, the $\Delta M = \pm 1$ transition corresponds to an energy splitting of

$$\Delta W_{\text{Stark}} = h\nu_0 = \frac{1}{2}\mu E \tag{4}$$

Therefore one obtains the resonant frequency

$$\nu_0 = {}^1/_2 \frac{\mu E}{h} \tag{5}$$

with $\nu_0 = \omega_0/2\pi$.

Thus, the resonant interaction referred to in the present work means the use of the RF frequency given by eq 5 which under the present conditions (see below) is 1411 kHz.

The resonance unit, schematically shown in Figure 2, is of the same type as that described earlier.[14,15] Essentially, it consists of two parallel Cu coated glass plates (length 10 cm along the beam, height 6 cm) separated by 0.67 cm. In one plate, a 1 mm wide scratch insulates electrically a rectangle of 8 cm by 3 cm; the rectangle and the rest of the plate form the electrodes to which the RF is applied. The static voltage is applied to the rectangular electrode and the opposite plate. The molecular beam runs parallel to the scratch (along the *x*-axis) 0.34 cm away

from the plate. At this distance, the homogeneous static field (z-axis) is perpendicular to the RF field (y-axis). Under the experimental conditions used in this investigation, the time the molecule spends inside the RF field is about 160 μs.

A movable slit was used to record the beam profile. The slit position can be changed by a computer controlled step motor by increments of 0.01 cm along the z-axis (i.e., perpendicular to the beam direction). Further experimental conditions are the same as those used in our previous work.[15]

The experimental procedure was the following: First, a static DC field of 1.49 kV/m was set into the two plates of the electric unit to produce a Stark splitting of 1411 kHz for the toluene $J = K = 1$ and $\Delta M = \pm 1$ transitions. Second, a nonresonant RF field of $\nu_{off} = 1300$ kHz was established in between the RF plates, with a field strength of 1.12 kV/m. The gradient of the RF field at the center of the beam was determined[23] to be -0.610 kV/m^2. Since the origin of the RF field, i.e., the horizontal scratch of the RF plate, is located toward the negative values of the slit position one should expect that the smaller the z the higher the E_1 value. In other words, the E_1 field along the z-axis is given by $E_1 = (1.12 - 0.610(z/\text{mm}))$ kV/m, where z should be given in mm. In this equation, a linear dependence of E_1 with z has been adopted which seems to be a good approximation as indicated in ref 16.

Finally, conditions were varied to turn the RF field to on resonance, $\nu_{on} = 1411$ kHz, with all experimental parameters, i.e., Stark, RF field, and radio frequency fixed and only the slit position was changed. Thus, the toluene signal intensity was monitored as a function of the slit position to record a transverse beam profile spectrum. A typical run consisted of averaging 100 laser shots for each on and off spectrum. Though the methodology employed in this work was the same as that in ref 15, the experimental conditions were optimized so as to obtain a better signal-to-noise ratio. Thus, with respect to our previous work, we used a higher and better controlled stagnation nozzle pressure, a higher number of laser shots for each slit position, and a wider interval of slit movement which for the present work ranged from -3 nm to $+3$ nm.

Results

Figure 3 shows the beam signal intensity as a function of the slit position. Two beam profiles are displayed at two distinct RF frequencies, 1300 kHz (off-resonance conditions) in the top panel and 1411 kHz (on-resonance conditions) in the bottom panel. A total of 100 laser shoots were averaged for each slit position, which was moved by 0.01 cm increments. To reduce possible effects due to signal drifts, one ON beam profile was followed by one OFF beam profile measurement and so on. Four runs under OFF and ON conditions were averaged to obtain the top and bottom profiles, respectively.

Interestingly, the total beam signal, i.e., the signal integral over the slit position, is, within the experimental error, the same for the two beam profiles. Looking at both off and on beam profiles, a peak structure is clearly manifested in the on beam profile which, however, is absent in the off beam profile. The structure consists of a series of peaks distributed at both positive and negative sides of the beam profile.

Data Analysis and Discussion

It is interesting to compare the present results with those obtained earlier in our laboratory[15] using the same technique and molecule. Both toluene transverse profiles are shown for comparison in Figure 4. The previous beam profile was taken under poorer experimental conditions as already explained in the experimental section. This was manifested by the lack of significant beam signal beyond ± 2 mm and by a poorer peak structure. Nevertheless, when the two profiles are normalized to each other, the consistency between them is manifested, as one can see how the earlier reported profile turns out to be a (low resolution) average of the presently measured profile.

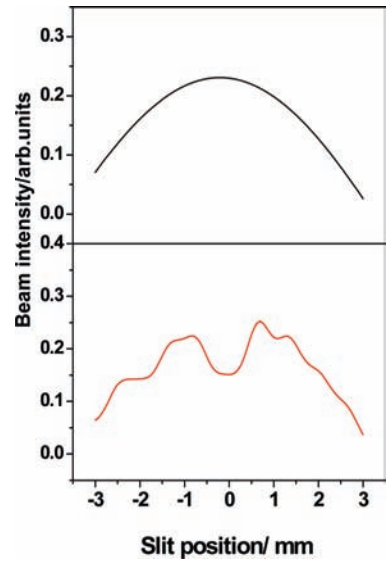

Figure 3. Toluene transverse beam profile as a function of the slit position: (top panel) OFF beam profile ($\nu_{off} = 1300$ kHz); (bottom panel) ON beam profile ($\nu_{on} = 1411$ kHz). Field conditions are $E = 14.18$ kV/m and $E_1 = 1.12$ kV/m. The relative units of the Y-axis are the same for both the upper and lower panels.

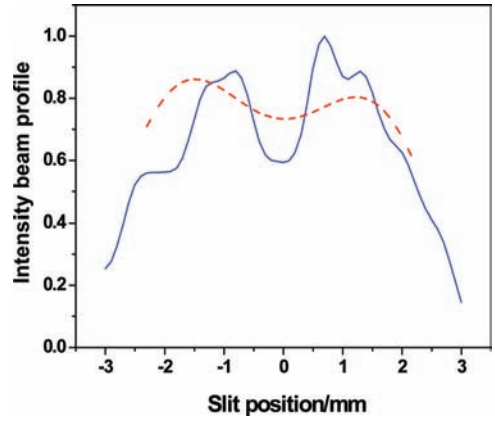

Figure 4. Transverse beam profile as a function of the slit position: (dashed line) ON beam profile from ref 15; (solid line) present results, i.e., those of the bottom panel from Figure 2.

Since the resonant RF field has a gradient of $\delta E/\delta z = -610$ kV/m^2, one could think the observed peak structure in the beam profile is due to Stern−Gerlach transverse beam deflection. The calculated beam deflection by the RF gradient is about 0.4×10^{-3} mn which is, at least, 3 orders of magnitude smaller than the experimentally observed peak spacing. Therefore, the peak structure of the beam profile cannot be attributed to beam deflection from the RF field gradient.

The interaction of the polar molecule with the resonant field was considered in a previous work[17] using a two-state model system. An important result of that work (see eqs 28−30 of ref 17) was that the beam signal can be expressed in the form

$$S = A + B\langle \cos \varphi_{ab} \rangle \qquad (6)$$

where A and B are related to the two-state wave functions, φ_{ab} is the phase shift introduced by the RF field, and t is the molecule−field interaction time. In the above equation, $\langle ... \rangle$ stands for the average value calculated using the experimental beam velocity distribution.

The resonant phase shift, φ^0_{ab}, was found to be[17]

$$\varphi^0_{ab} = \Omega_R t(\sin \Omega_R t \sin 2\omega_0 t) \quad (7)$$

where Ω_R stands for the Rabi frequency of the transitions and ω_0 is the applied resonant angular frequency.

Since the Rabi frequency is given by[19]

$$\Omega_R = \frac{\mu_{12} E_1}{\hbar} \quad (8)$$

with μ_{12} being the transition moment between the two (J, K, M) states coupled by the resonant field; the experimentally introduced z-gradient in E_1 produces a change in the phase shift along the z-direction and, consequently, a change in the beam signal. In other words, the molecular interferences in the transverse beam profile are clearly a consequence of the oscillatory behavior of the phase shift due to the change of the resonant field amplitude along the z-direction. More explicitly, one could write eq 6 in the form

$$S(z) = A + B\langle \cos \varphi_{ab}(z) \rangle \quad (9)$$

$$\text{with} \quad \varphi_{ab}(z) = aE_1(z) \sin(bE_1(z)) \quad (10)$$

with z being the perpendicular direction to the beam propagation axis and a and b z-independent parameters.

The simulation using the Simion software indicates the RF field strength values around the central part of the RF unit can be well described by a linear dependence on z. Thus, one can write

$$E_1(z) = E_1(0) + E'_1(z) \quad (11)$$

$$\text{with} \quad E'_1 = \delta E_1/\delta z \quad (12)$$

By replacing eq 11 in eq 10, one reaches the conclusion that for $E'_1 = 0$ the phase shift shows no z dependence. In other words, the observed fringes in the transverse beam profile are due to the gradient of the RF field such that the higher the gradient the larger the number of fringes.

The calculated beam profile is the convolution of the signal, given by eq 6, with the molecular beam velocity distribution given by

$$f(v) = N\frac{v^2}{\sigma^3} \exp[-(v - v_0)^2/\sigma^2] \quad (13)$$

Here, N is the normalization constant, v_0 is the peak velocity, and σ is related to the width of the distribution. Figure 5 shows the best fit to the experimental beam profile which was obtained with a peak velocity of $v_0 = 550$ m/s, $\sigma = 40$ m/s, a RF frequency of $\nu_0 = 1411$kHz, and a RF field of $E_1 = (0.02 - 0.004(z/\text{mm}))$ kV/m. Furthermore, the slit broadening effects were also taken into account.

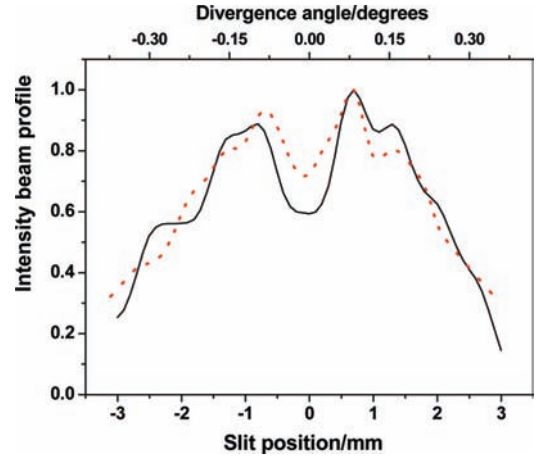

Figure 5. Comparison between experimental and calculated ON profiles. The solid line shows the experimental results (same as Figure 2, bottom panel). The dotted line is the calculated beam profile using eq 9 of the text with the best fit parameters described in the Data Analysis and Discussion section. While the bottom axis refers to the slit position in mm, the upper one refers to the divergence angle taking the beam direction as 0°. Both profiles are normalized to 1 at the peak.

Inspection of Figure 5 indicates the simulated profile reproduces satisfactorily the main features of the experimental one. In addition to the full width at half-maximum, the minimum at $z = 0$ mm and the four main peak locations, two at each side of the beam propagation direction, are well reproduced. Except for the RF field amplitude, the input values employed in the simulation are those of the experiment. However, the best fit value of $E_1 = (0.02 - 0.004(z/\text{mm}))$ kV/m is significantly smaller than the nominal E_1 value (inside the C-field). At present, we cannot offer a full explanation for such a difference. Nevertheless, we shall consider the ionization region is situated 21 cm from the C-field, as illustrated in Figure 1. After the molecular beam exits the RF unit, the resonant field is no longer interacting with the dipole moment and quantum decoherence is taking place. Due to the low background pressure ($<10^{-6}$ Torr), and even assuming a toluene elastic cross section of 1000 Å^2, the estimated average number of collisions along the 21 cm distance the beam travels before it is detected is less than 0.1 collisions. Thus, decoherence due to background scattering is playing a minor role at least under our experimental conditions, suggesting other decoherence mechanisms responsible for the small best fit E_1 value.

Precisely, the suggested decoherence hypothesis opens the way for future investigations aimed at studying the decoherence mechanisms of these molecular beams by monitoring the evolution of fringes' visibility as a function of the molecule−field interaction time. Work is now in progress along this direction.

Summary and Conclusions

In this work, measurements on the toluene beam signal intensities recorded by laser ionization coupled with time-of-flight mass spectrometry were reported. The beam signal was measured after the beam passed through a RF unit in which these molecules interact with both static DC and oscillating RF electric fields. The measurements clearly demonstrate how the interaction of a resonant RF field with the polar toluene molecule produces a series of peaks in the

transverse beam profile that can be rationalized by the onset of molecular interferences.

The major relevance of the present work is the observation of an interferogram structure in the transverse toluene beam profile when it resonantly interacts with a RF field. While in ref 15 only a molecular beam splitting toward both sizes of the transverse beam axis was observed, in the present work, a peak structure was clearly resolved as a result of better experimental conditions and higher resolution.

What should be also pointed out is the satisfactory rationalization of the observed profile structure by the molecular interference model reported in ref 17. The key ingredient of the theoretical model is the resonant interaction between the RF field and the molecular dipole moment. Only under resonant conditions this interaction is non-negligible and, which is more important, different for each (J, K, M) state coupled by the resonant field. It was demonstrated that the observed peak structure of the transverse beam profile is a manifestation of the phase shift variation along the perpendicular beam direction which, in turn, is due to the change of the RF field strength along this direction.

Finally, it is interesting to remark how the employed resonant RF electric unit, a simple device widely used in early molecular beam electric resonance experiments,[24] seems to be adequate to investigate new possibilities in molecular interferometry. In this sense, a possibility we are also considering for future work is the measurement of the beam profile after the beam travels through a scattering cell to investigate the extent of the collisional decoherence[25] by monitoring the fringe visibility as a function of the scattering gas nature and pressure. Certainly, the present simple molecular beam technology seems to be very promising to investigate the quantum control of molecular processes using RF fields.

Acknowledgment. Financial support from the Ministerial de Educación y Ciencia of Spain (grant CTQ2007-61749) is gratefully acknowledged. J.O.C. acknowledges a Ramón y Cajal Research Contract from The Ministerio de Educación y Ciencia of Spain. A.G.G. acknowledges a FPI fellowship from the MICINN of Spain.

References and Notes

(1) Estermann, I.; Stern, O. *Z. Phys.* **1930**, *61*, 95.
(2) Bordé, C.; Courtier, N.; Burck, F. D.; Goncharov, A.; Gorlicki, M. *Phys. Lett. A* **1994**, *188*, 187.
(3) Lisdat, C.; Frank, M; Knockle, H.; Almanzor, M. L.; Tiemann, E. *Eur. Phys. J. D* **2000**, *12*, 235.
(4) Chapman, M. S.; Ekstrom, C. R.; Hamnond, T. D.; Rubestein, R. A.; Schmiedmayer, J.; Wehinger, S.; Prichard, D. E. *Phys. Rev. Lett.* **1995**, *74*, 4783.
(5) Clauser, J. F.; Li, S. Generalized Talbot-Lau Atom Interferometry. In *Atom Interferometry*; Berman, P. R., Ed.; Academic Press: San Diego, CA, 1997.
(6) Schöllkopf, W.; Toennies, J. P. *J. Chem. Phys.* **1996**, *104*, 1155.
(7) Grisenti, R. E.; Schöllkopf, W.; Toennies, J. P.; Hegerfeldt, G. C.; Kohler, T.; Stoll, M. *Phys. Rev. Lett.* **2000**, *85*, 2284.
(8) Bruch, L. W.; Schollkopf, W.; Toennies, J. P. *J. Chem. Phys.* **2002**, *117*, 1544.
(9) Nairz, O.; Amdt, M.; Zeilinger, A. *Am. J. Phys* **2003**, *71*, 319.
(10) Brezger, B.; Hackermuller, L; Utternthaler, S.; Petschinka, J.; Arndt, M.; Zeilinger, A. *Phys. Rev. Lett.* **2002**, *88*, 100404.
(11) Montero, C.; González Ureña, A.; Caceres, J. O.; Morato, M.; Najera, J.; Loesch, H. J. *Eur. Phys. J. D* **2003**, *26*, 261.
(12) Morato, M.; Gasmi, K.; Montero, M.; González Ureña, A. *Chem. Phys. Lett.* **2004**, *392*, 255.
(13) Caceres, J. O.; Montero, C.; Morato, M.; González Ureña, A. *Chem. Phys. Lett.* **2006**, *426*, 214.
(14) Morato, M.; Cáceres, J. O.; González Ureña, A. *Eur. Phys. J. D* **2006**, *38*, 215.
(15) Morato, M.; Cáceres, J. O.; González Ureña, A. *Eur. Phys. J. D* **2006**, *39*, 199.
(16) González Ureña, A.; Cáceres, J. O.; Morato, M. *Chem. Phys.* **2006**, *328*, 156.
(17) González Ureña, A.; Requena, A.; Bastida, A.; Zuñiga, J. *Eur. Phys. J. D* **2008**, *49*, 297.
(18) The nominal full beam divergence $\Delta\theta$ was estimated on the basis of the beam geometry and collimation from the last slit position considering the nozzle as a virtual point. Thus, $\Delta\theta = 2x \tan^{-1}(0.7 \text{ mm}/480 \text{ mm}) \approx 2.8 \times 10^{-3}$ rad.
(19) Ramsey, N. F. *Molecular Beams*; Oxford University Press: Oxford, U.K., 1956. See also: Bransder, B. H.; Joachain, C. J. *Physics of Atoms and Molecules*; Longman: London, U.K., 1983; p 558.
(20) Van Vleck, J. H. *The Theory of Electric and Magnetic Susceptibilities*; Oxford University Press: Oxford: U.K., 1932.
(21) Herzberg, G. *Molecular Spectra and Molecular Structure. Vol. I. Spectra of Diatomic Molecules*; Van Nostrand Reinhold Company: New York, 1950; p 307.
(22) *Handbook of Chemistry and Physics*, 74th ed.; Chemical Rubber Publishing Company: Cleveland, OH, 1993−1994.
(23) The calculation was done using the Simion 7.0 program.
(24) Trischka, J. W. *Phys. Rev.* **1948**, *74*, 718.
(25) Hornberger, K.; Uttenthaler, S.; Brezger, B.; Hackermüller, L.; Arndt, M.; Zeilinger, A.; *Phys. Rev. Lett.* **2003**, *90*, 160401.

JP902928E